Decoupling Classifier for Boosting Few-shot Object Detection and Instance Segmentation

Anonymous Author(s)
Affiliation
Address
email

Abstract

This paper focus on few-shot object detection (FSOD) and instance segmentation (FSIS), which requires a model to quickly adapt to novel classes with a few labeled instances. The existing methods severely suffer from bias classification because of the missing label issue which naturally exists in a few-shot scenario and is first formally proposed by us. Our analysis suggests that the standard classification head of most FSOD or FSIS models needs to be decoupled to mitigate the bias classification. Therefore, we propose an embarrassingly simple but effective method that decouples the standard classifier into two heads. Then, these two individual heads are capable of independently addressing clear positive samples and noisy negative samples which are caused by the missing label. In this way, the model can effectively learn novel classes while mitigating the effects of noisy negative samples. Without bells and whistles, our model without any additional computation cost and parameters consistently outperforms its baseline and state-of-the-art by a large margin on PASCAL VOC and MS-COCO benchmarks for FSOD and FSIS tasks. The code will be available.

1 Introduction

Fully supervised deep convolutional neural network have achieved remarkable progress on various computer vision tasks, such as image classification [12], object detection [9, 3, 23], semantic segmentation [18, 2] and instance segmentation [11] in recent years. However, the superior performance heavily depends on a large amount of annotated images. In contrast, humans can quickly learn novel concepts from a few training examples. To this end, a few-shot learning paradigm [7] is presented, and its goal aims to adapt novel classes when only providing a few labeled examples. Unfortunately, existing few-shot models are still far behind humans, especially for few-shot object detection (FSOD) and few-shot instance segmentation (FSIS).

Various methods have been proposed to tackle the problem of the FSOD and FSIS. The earlier works [27, 31] mainly follow meta-learning paradigm to acquire task-level knowledge on base classes and generalize better to novel classes. However, these methods usually suffer from a complicated training process (episodic training) and data organization (support query pair). The recent transfer-learning (fine-tuning) methods [26, 28, 25, 1, 21] significantly outperforms the earlier meta-learning ones. Furthermore, it is more simple and efficient. These fine-tuning methods mainly use fully supervised object detection or instance segmentation framework, e.g., Faster-RCNN [24] or Mask-RCNN [11]. Therefore, it may be suboptimal for few-shot scenario.

The PASCAL VOC [4] and MS-COCO [17] are widely used to evaluate the performance of object detection or instance segmentation. Under a fully supervised setting, the model can be well-trained on these two datasets because all interest objects are almost completely labeled. Under a few-shot scenario, however, we find that there is a large number of instances that are missing annotations as

Submitted to 36th Conference on Neural Information Processing Systems (NeurIPS 2022). Do not distribute.

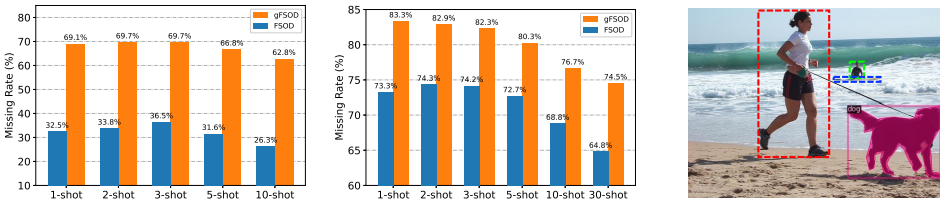

(a) PASCAL VOC (b) MS-COCO (c) a one-shot labeled image

Figure 1: The proportion of missing instances in the training set for FSOD and gFSOD on (a) PASCAL-VOC and (b) MS-COCO datasets. It can be observed that there is a high missing rate in each shot, especially for the gFSOD. In (c), two "person" instances present in the one-shot labeled image, but they are mislabeled.

shown in Fig. 1 (detailed discussion in Sec. 3.2). Therefore, it may result in biased classification and thus limit the generalization ability of novel classes using the model trained on these mislabeled datasets if we don't take any action.

Recent FSCE [25] overcomes the misclassification with contrastive proposal encoding loss. DeFRCN [21] alleviates the foreground-background confusion between base pre-training and novel fine-tuning with task decoupling. Unlike these works, we propose a simple decoupling method to mitigate the biased classification issue. Specifically, we firstly decouple the standard classifier into two parallel heads, positive and negative ones. Then, these two heads independently process positive and negative samples with different strategies. Our contributions are summarized as follows:

- We rethink FSOD and FSIS from the perspective of label completeness and discover that existing fine-tuning learning-based few-shot methods severely suffer from bias classification because the missing label issue naturally exists in the few-shot scenarios. To be best of our knowledge, this is the first to propose missing label issue in FSOD and FSIS.
- To mitigate the bias classification, we propose a simple but effective method that decouples the standard classifier into two parallel heads to independently process clear positive samples and noisy negative ones. Without bells and whistles, the proposed decoupling classifier can be taken as an alternative to the standard classifier in state-of-the-art FSOD or FSIS models.
- Comprehensive experimental results on PASCAL VOC and MS-COCO show that our approach without any additional parameters and computation cost outperforms state-of-the-art both on FSOD and FSIS tasks.

2 Related Work

FSOD aims to recognize novel objects and localize them with bounding boxes when only providing a few training instances on each novel class. Existing works can be roughly grouped into two families, meta-learning and transfer-learning, according to training paradigm. The meta-learning methods [27, 14, 31, 5, 30, 15, 16, 32, 13, 10] use episodic training to acquire task-level knowledge on base classes and generalize better to novel classes. The transfer-learning methods [26, 28, 25, 32, 1, 21] generally utilize two-stage training strategy first pre-training on base classes and then fine-tuning on novel classes, which have significantly outperformed many earlier meta-learning approaches. Recent FSCE [25] shows that the degradation of detection performance mainly comes from misclassifying novel instances as confusable classes, and they propose a contrastive proposal encoding loss to ease the issue. Similar to the FSCE, FADI [1] explicitly associates each novel class with a semantically similar base class to learn a compact intra-class distribution. DeFRCN [21] decouples Faster-RCNN [24] to alleviate the foreground-background confusion between pre-training and fine-tuning stage.

FSIS needs to not only recognize novel objects and their location but also perform pixel-level semantic segmentation for each detected instance. Many FSIS approaches typically use the FSOD framework, e.g., Mask-RCNN [11], it is built on the Faster-RCNN by adding a mask segmentation head. Therefore, most FSIS methods generally follow the FSOD learning paradigm, i.e., meta-learning [19, 31, 6, 20] or transfer-learning [8]. Siamese Mask-RCNN [19] and Meta-RCNN [31] commonly compute embeddings of support images and combine these with those features produced

by a backbone network. Their difference is the combination strategy, e.g., subtraction in [19] and concatenation in [31]. These works only focus on the performance of novel classes and ignore that of base classes. In real-world applications, we expect that one few-shot model not only recognizes novel classes but also remembers base classes. The recent iMTFA [8] introduces incremental learning into FSIS and propose incremental FSIS task.

3 Methodology

3.1 Few-shot Object Detection and Instance Segmentation Setting

Given an image dataset $D = \{X_i, Y_i\}_{i=1}^{N}$, where X_i denotes the i-th image and Y_i is its corresponding annotation. For object detection, Y_i=$\{b_k, c_k\}_{k=1}^{M}$, where b_k and c_k represent bounding box coordinates and category of the k-th instance presented image X_i, respectively. For instance segmentation, Y_i includes pixel-level mask m_k annotation beyond category and bounding box ones, i.e., Y_i=$\{b_k, m_k, c_k\}_{k=1}^{M}$. Under few-shot learning setting, these annotations can be grouped into two sets, base and novel classes, denoted as C_{base} and C_{novel}. Note, the base and novel classes are non-overlapping (i.e., $C_{base} \cap C_{novel} = \emptyset$).

FSOD or FSIS aims to detect/segment novel class instances through training a model based on plenty of labeled instances on a set of base classes and a few instances (e.g, 1, 2, 3 and 5) on each novel class. Note, FSOD or FSIS only focuses on recognizing novel class instances but ignores base class ones. It is impractical from the perspective of many real-world applications because ones always expect that a few-shot model is capable of not only recognizing novel classes but also remembering base classes. To this end, generalized FSOD and FSIS (abbreviated as gFSOD and gFSIS) requires a model to adapt to novel classes without forgetting its existing knowledge (base classes).

As mentioned above, the transfer-learning-based FSOD and FSIS methods mainly consist of two stages, i.e., pre-training on base classes and fine-tuning on novel classes. The former is trained on plenty of labeled instances in C_{base} while the latter only uses a few labeled instances in C_{novel}. For generalized few-shot learning, the main difference is novel stage training which uses few labeled instances in both C_{base} and C_{novel}. Note that the labeled instances are abundant at the base stage, but there are only a few labeled instances for at novel stage no matter FSOD/FSIS or gFSOD/gFSIS. Therefore, most instances are unlabeled (missing labeled) as only K instances are provided at the fine-tuning stage. This is reasonable from the perspective of data privacy (incremental learning).

3.2 Revisiting Object Detection and Instance Segmentation

We focus on fine-tuning based FSOD and FSIS because it is more simple and effective compared to meta based ones. As we know, Faster-RCNN and Mask-RCNN are very popular and powerful solutions as two-stage stacking architecture for fully supervised object detection and instance segmentation. We firstly describe the two-stage detector and segmenter. In general, the first stage is designed to generate class-agnostic region proposals which can be formulated as:

$$\mathcal{F}_{\mathrm{s1}}(\theta_{s1}; \cdot) = \mathcal{F}_{\mathrm{ROI}} \circ \mathcal{F}_{\mathrm{RPN}} \circ \mathcal{F}_{\mathrm{EF}}(\cdot), \tag{1}$$

where the θ_{s1} is all the parameters of the first stage. Specifically, an input image X_i is firstly fed into a backbone network to Extract high-level Features ($\mathcal{F}_{\mathrm{EF}}$). Then, a Region Proposal Network (RPN) is adopted to generate candidate regions based on these extracted features ($\mathcal{F}_{\mathrm{RPN}}$). Finally, all these region proposals are pooled into a fixed size feature map using a Region of Interest pooling module ($\mathcal{F}_{\mathrm{ROI}}$) for the following stage. The structure of the second stage varies depending on the specific task. For object detection, the ROI features of *sampled* region proposals will be parallelly fed into two heads for performing box classification and regression, that is

$$\mathcal{L}_{\mathrm{s2}}^{\mathrm{OD}} = \mathcal{L}_{\mathrm{CLS}}(\theta_{cls}; \cdot) + \mathcal{L}_{\mathrm{REG}}(\theta_{reg}; \cdot), \tag{2}$$

where θ_{cls} and θ_{reg} are the parameters of classification and regression head, respectively. Instance segmentation method (e.g., Mask-RCNN) follows the second stage structure of object detection and applies it to three heads, i.e., box classification, box regression and mask segmentation, that is

$$\mathcal{L}_{\mathrm{s2}}^{\mathrm{IS}}(\cdot) = \mathcal{L}_{\mathrm{CLS}}(\theta_{cls}; \cdot) + \mathcal{L}_{\mathrm{REG}}(\theta_{reg}; \cdot) + \mathcal{L}_{\mathrm{SEG}}(\theta_{seg}; \cdot), \tag{3}$$

where θ_{seg} is parameters of the mask segmentation head. Given an input image X_i and its corresponding annotation Y_i=$\{b_k, c_k\}_{k=1}^{M}$ or Y_i=$\{b_k, m_k, c_k\}_{k=1}^{M}$, Eqs. 2 and 3 can be jointly optimized

end-to-end by minimizing $\mathcal{L}_{\mathrm{s2}}^{\mathrm{OD}}(\cdot)$ and $\mathcal{L}_{\mathrm{s2}}^{\mathrm{IS}}(\cdot)$, which follows a multi-task learning paradigm. Note, we omitted the RPN learning in Eqs. 2 and 3 for simplicity.

Missing Label Issue. We can obtain a powerful model minimizing Eqs. 2 and 3 when all interesting instances are completely labeled in a large-scale image dataset D. The completeness of annotation at label space is, in fact, a general precondition for most fully supervised learning algorithms. However, it is not satisfactory for a few-shot learning scenario. The reason is that only a few instances are manually labeled in given training images, and a lot of potential instances may be presented but unlabeled. From the perspective of practical application, it is natural and unavoidable to miss annotations when facing a few-shot setting. As shown in Fig. 1 (c), we can see that there are at least three instances including two "person" and one "dog" in this image, but only the "dog" instance carrying annotation (box, mask, category), and other two "person" instances are unlabeled (i.e., missing labels).

In order to quantitatively measure the proportion of missing labeled instances, we compute the average missing rate for each shot on PASCAL VOC and MS-COCO benchmark datasets as shown in Fig. 1. Firstly, it can be seen that there is a high missing rate on each shot. For example, 74.3% novel class instances potentially present on 3-shot MS-COCO training images, but they are not given any annotations. Secondly, the missing rate is further increased under a generalized few-shot setting. For example, the missing rate increases nearly two times of few-shot setting on the PASCAL VOC. Despite some efforts try mining these missing labeled instances in a semi-supervised manner for boosting few-shot performance, the fully supervised loss with Eqs. 2 and 3 may result in a suboptimal solution when some instances are unlabeled. To be best of our knowledge, this is the first to propose the missing label issue in few-shot object detection and instance segmentation.

Biased Classification Issue. The Eqs. 2 and 3 can be optimized using sampled ROI features and their labels as mentioned above. The sampling operation performs box matching between "ROI features" and "annotation", and assigns training labels (positive or negative) to the corresponding ROIs. Here, the positive (foreground) ROIs are sampled from object proposals that have an IoU overlap with the ground-truth bounding box at a threshold (e.g., 0.5), while negative (background) ROIs are sampled from the remaining proposals. The classification head is trained based on these sampled positive and negative ROIs. Different from the classification head, the box regression, and mask segmentation head learning are only associated with positive ROIs.

The annotations of positive ROIs are accurate, e.g., the annotations of the "dog" instances in Fig. 1 (c). However, the sampled negative ROIs may be noisy because of the missing label issue under the few-shot setting. For example, those two "people" instances will be assigned to negative labels (i.e., background) if they are sampled in Fig. 1 (c), according to the above label assignment strategy. This will make the standard classification head confused with positive and negative samples. On one hand, the model is correctly guided to recognize positive objects because all positive samples are accurate. On the other hand, the model may be misguided by noisy negative samples and thus recognize positive objects as background. Therefore, the bias classification may happen when meeting the missing label issue, especially in a few-shot scenario. Furthermore, it potentially limits the generalization ability to adapt to the novel class quickly and efficiently.

3.3 Decoupling Classifier to Mitigate the Bias Classification

Standard Classifier. We assume that $\boldsymbol{x} \in \mathbb{R}^{C+1}$ is the predicted logit of a sampled ROI feature obtained from Eq. 1 and its corresponding class label vector is $\boldsymbol{y} \in \mathbb{R}^{C+1}$, where there are C foreground categories and one background class, and y_i is 1 if the corresponding proposal belongs to the i-th category, 0 otherwise. Then, we use a softmax function to transform it into a probability distribution, that is

$$\hat{p}_i = \frac{\exp(x_i)}{\sum_t \exp(x_t)}. \tag{4}$$

The cross entropy loss is used as the measurement of the similarity between the ground-truth $\boldsymbol{y}$ and predicted distribution $\hat{\boldsymbol{p}}$, that is

$$\mathcal{L}_{\mathrm{CLS}} = -\sum_{i=1}^{C+1} y_i \log(\hat{p}_i) \tag{5}$$

Note that the standard classifier (Eqs. 4 and 5) may confuse with clear positive and noisy negative samples in few-shot scenario.

Decoupling Classifier. In order to process positive and negative samples differentially, we decouple the standard classifier into two heads, i.e., positive (foreground) and negative (background) heads, which are formulated as

$$\mathcal{L}_{\mathrm{CLS}} = \mathcal{L}_{\mathrm{CLS}}^{\mathrm{fg}} + \mathcal{L}_{\mathrm{CLS}}^{\mathrm{bg}} \tag{6}$$

Here, the positive and negative heads are responsible for positive and negative samples, respectively. Considering that the labels of positive samples (foreground) are accurate, we can use the cross entropy loss (i.e., Eq. 5) for all positive instances. The labels of those negative examples may be noisy because the missing label issue. Therefore, it is not reasonable to employ normal cross entropy loss for training the negative head. Note that these negative examples are generally sampled from those object proposals that have a maximum IoU overlap with the ground truth bounding box at an interval $[0, 0.5)$, and thus we can infer that they may not belong to the ground truth class, although we don't know their true category. We expect that the bias classification would be mitigated if the negative head performs learning only between few-shot labeled categories and the background class. To this end, we first collect all category labels of a few-shot labeled image, and denote it as $\boldsymbol{m}$=$[m^1, m^2, \cdots, m^C, m^{C+1}]^T$, where m^i is a binary indicator, and m^i is 1 if the image is labeled with the i-th category, 0 otherwise. Note that m^{C+1}=1 indicates that each image at least contains a background class. Then, we can obtain a constrained logit $\bar{\boldsymbol{x}}$ conditioned on the $\boldsymbol{m}$, that is

$$\bar{x}_i = m_i x_i. \tag{7}$$

Substituting Eq. 7 into the softmax function Eq. 4 yields:

$$\bar{p}_i = \frac{\exp(m_i x_i)}{\sum_t \exp(m_t x_t)}. \tag{8}$$

We compute cross entropy loss between $\bar{\boldsymbol{p}}$ and the corresponding ground truth $\boldsymbol{y}^{\mathrm{bg}}$, that is

$$\mathcal{L}_{\mathrm{CLS}}^{\mathrm{bg}} = -\sum_{i=1}^{C+1} y_i^{\mathrm{bg}} \log(\bar{p}_i), \tag{9}$$

where y_{C+1}^{bg}=1 and $y_{i \neq C+1}^{\mathrm{bg}}$=0.

Optimization with the Decoupling Classifier. Considering the joint optimization goal (Eq. 2 and 3) of object detection and instance segmentation, the optimal parameters Θ is determined by minimizing Eq. 2 and 3, where $\Theta = \{\theta_{s1}, \theta_{cls}, \theta_{reg}\}$ in object detection, and $\Theta = \{\theta_{s1}, \theta_{cls}, \theta_{reg}, \theta_{seg}\}$ in instance segmentation. For simplicity, we only consider the optimization for the classification head and omitted the box regression and mask segmentation head in the following analysis. θ_{cls} is updated by a gradient descent step, that is

$$\theta_{cls} \leftarrow \theta_{cls} - \lambda \frac{\partial \mathcal{L}_{cls}}{\partial \theta_{cls}}, \tag{10}$$

where λ is the learning rate. Note that we have decoupled the standard classifier into positive and negative learning in Eq. 6. We firstly analyze the θ_{cls} optimization for positive head. According to the chain rule in Eq. 4 and 5, we have

$$\frac{\partial \mathcal{L}_{cls}}{\partial \boldsymbol{x}} = \hat{\boldsymbol{p}} - \boldsymbol{y}^{\mathrm{fg}}. \tag{11}$$

Then, the derivative of L_{cls}^{fg} with respect to θ_{cls} is

$$\frac{\partial \mathcal{L}_{cls}}{\partial \theta_{cls}} = (\hat{\boldsymbol{p}} - \boldsymbol{y}^{\mathrm{fg}}) \frac{\partial \boldsymbol{x}}{\theta_{cls}}. \tag{12}$$

Combining the negative head in Eq. 9 and Eqs. 8 and 7, we can similarly obtain derivative of L_{cls}^{bg} with respect to θ_{cls} is

$$\frac{\partial \mathcal{L}_{cls}}{\partial \theta_{cls}} = \boldsymbol{m}(\bar{\boldsymbol{p}} - \boldsymbol{y}^{\mathrm{bg}}) \frac{\partial \boldsymbol{x}}{\theta_{cls}}, \tag{13}$$

where $\boldsymbol{y}^{\mathrm{bg}}$ is the ground truth label vector of a negative sample. Comparing Eqs. 12 with 13, we can see that the parameters θ_{cls} of the classification head will be updated with different ways for positive and negative examples. For the positive head, the gradient is updated in each dimension of the class space. But for the negative head, the gradient is limited in some special dimension because of introducing $\boldsymbol{m}$ and thus the biased classification may be alleviated.

In order to further understand Eqs. 12 and 13, we give a visualization example for decoupling classifier as illustrated in Fig. 2. Note that we use Gaussian normal distribution for prediction and ground truth distribution for intuition. Here, we take the one-shot labeled image in Fig. 1 (c) for example, where only the "dog" instance is labeled. We assume that one "person" instance is sampled as negative sample, and it will be mistaken as background class (ground truth). Due to the proposed decoupling classifier, the optimization of the "person" instance is constrained between the "dog" and "background" as shown in Fig. 2 (b) and doesn't affect the predictions of other categories such as the "person" class.

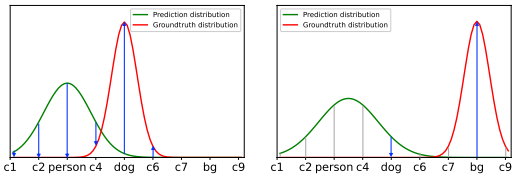

(a) Positive head (b) Negative head

Figure 2: Illustration of the gradient of decoupling classifier, where the blue arrow represents the gradient direction. (a) illustrates the gradient propagation on the positive head, and (b) reveals that the gradient propagation is constrained between few-shot labeled class (e.g., dog) and the background and thus the bias classification is mitigated. Best viewed in color and zoom in.

4 Experiments

In this section, we empirically evaluate the proposed method for FSOD/gFSOD and FSIS/gFSIS tasks and demonstrate its effectiveness by comparison with state-of-the-art methods.

4.1 Experimental Setup

Datasets. We follow the previous work and evaluate our method on PASCAL-VOC [4] and MS-COCO [17] datasets. For a fair comparison, we use the same data splits given in [26, 21].

PASCAL VOC covers 20 categories, which are randomly split into 15 base classes and 5 novel classes. There are three such splits in total. In each class, there are K (1, 2, 3, 5, 10) objects for few-shot training. And the PASCAL VOC 2007 testing set is used for evaluation. The dataset is only used to evaluate the FSOD. We report the Average Precision (IoU=0.5) for novel classes (AP50).

MS-COCO contains 80 classes. The 20 categories presented in the PASCAL VOC are used as novel classes and the remaining 60 categories are used as base classes. We train a few-shot model based on K (1, 2, 3, 5, 10, 30) instances for each class and evaluate on the MS-COCO validation set. This dataset has been widely used to evaluate the performance of FSOD and FSIS. We report Average Precision (IoU=0.5:0.95), Average Precision (IoU=0.5) on novel classes for FSOD and FSIS settings. In addition, we also report AP and AP50 for overall classes, base classes, and novel classes under gFSOD and gFSIS settings, respectively.

Experimental Details. The experiments are conducted with Detectron2 [29] on NVIDIA GPU V100 on CUDA 11.0. We use standard Faster-RCNN with ResNet-101 backbone extracted features from the final convolutional layer of the 4-th stage for few-shot object detection as the same as DeFRCN [21]. For instance segmentation, we add a mask prediction head at the ROI of the Faster-RCNN. For model training, we employ a two-stage fine-tuning approach: first training the network on the base classes with pre-trained by ImageNet and then fine-tuning on K-shots for every class. The SGD is used to optimize our network end-to-end with a mini-batch size of 16, momentum 0.9, and weight decay $5e^{-5}$ on 8 GPUs. The learning rate is set to 0.02 during base training and 0.01 during few-shot fine-tuning. Following the previous work [26], all experimental results are averaged over 10 seeds. For the FSOD, we also report the average results over 10 times repeated runs on `seed0` as the same as DeFRCN [22].

Strong Baseline. We compare our method with the state-of-the-art DeFRCN [21] for FSOD. For FSIS, we extend DeFRCN similarly to how Mask-RCNN extends Faster-RCNN, i.e., adding a mask prediction head at the ROI of the DeFRCN and keeping others as the same as DeFRCN, and thus we call it Mask-DeFRCN. Our method only replaces the standard classifier in DeFRCN and Mask-DeFRCN with our decoupling classifier. Therefore, DeFRCN and Mask-DeFRCN can be taken as our strong baseline for FSOD/gFSOD and FSIS/gFSIS tasks.

4.2 Comparison with the State-of-the-Art

Few-shot Instance Segmentation on the MS-COCO. *Our method (simple decoupling classifier) outperforms the state-of-the-art on the MS-COCO in either FSIS or gFSIS setting.* The main results

Table 1: FSIS performance (AP and AP50) for Novel classes on MS-COCO. The superscript † indicates that the results are our re-implementation. Note that our results are averaged over all 10 seeds and the best results are in bold, the same below.

Methods		Tasks	1		5		10		2		3		30	
			AP	**AP50**	**AP**	**AP50**	**AP**	**AP50**	**AP**	**AP50**	**AP**	**AP50**	**AP**	**AP50**
Meta R-CNN [31]	*ICCV 19*	Det	-	-	3.5	9.9	5.6	14.2	-	-	-	-	-	-
MTFA [8]	*CVPR 21*		2.47	4.85	6.61	12.32	8.52	15.53	-	-	-	-	-	-
iMTFA [8]	*CVPR 21*		3.28	6.01	6.22	11.28	7.14	12.91	-	-	-	-	-	-
Mask-DeFRCN† [21]	*ICCV 21*		7.54	14.46	15.39	27.29	18.72	32.80	11.01	20.20	13.07	23.28	22.63	38.95
Ours			**8.09**	**15.85**	**16.39**	**29.96**	**19.33**	**34.78**	**11.90**	**22.39**	**14.04**	**25.74**	**22.73**	**40.24**
Meta R-CNN [31]	*ICCV 19*	Seg	-	-	2.8	6.9	4.4	10.6	-	-	-	-	-	-
MTFA [8]	*CVPR 21*		2.66	4.56	6.62	11.58	8.39	14.64	-	-	-	-	-	-
iMTFA [8]	*CVPR 21*		2.83	4.75	5.24	8.73	5.94	9.96	-	-	-	-	-	-
Mask-DeFRCN† [21]	*ICCV 21*		6.69	13.24	12.66	24.58	15.39	29.71	11.01	9.51	11.01	21.27	18.28	35.20
Ours			**7.18**	**14.33**	**13.48**	**26.67**	**15.85**	**31.33**	**11.90**	**10.31**	**11.85**	**23.24**	**18.34**	**35.99**

Table 2: gFSIS performance (AP and AP50) for Overall, Base and Novel classes on MS-COCO.

Shots	Methods	**Object Detection**						**Instance Segmentation**					
		Overall		**Base**		**Novel**		**Overall**		**Base**		**Novel**	
		AP	**AP50**	**AP**	**AP50**	**AP**	**AP50**	**AP**	**AP50**	**AP**	**AP50**	**AP**	**AP50**
	Base-Only			39.86	59.25					32.58	55.12		
1	iMTFA [8]	21.67	31.55	27.81	40.11	3.23	5.89	20.13	30.64	25.90	39.28	2.81	4.72
	Mask-DeFRCN	23.82	35.70	30.11	44.42	4.95	9.55	19.58	33.38	24.63	41.57	4.45	8.81
	Ours	**27.35**	**42.55**	**34.35**	**52.46**	**6.34**	**12.79**	**22.45**	**39.33**	**28.03**	**48.60**	**5.72**	**11.53**
5	iMTFA [8]	19.62	28.06	24.13	33.69	6.07	11.15	18.22	27.10	22.56	33.25	5.19	8.65
	Mask-DeFRCN† [21]	27.82	42.12	32.54	48.03	13.69	24.41	23.03	39.37	26.84	45.04	11.60	22.36
	Ours	**30.48**	**47.75**	**35.30**	**53.65**	**16.02**	**30.05**	**25.20**	**44.12**	**29.10**	**49.87**	**13.50**	**26.86**
10	iMTFA [8]	19.26	27.49	23.36	32.41	6.97	12.72	17.87	26.46	21.87	32.01	5.88	9.81
	Mask-DeFRCN† [21]	29.88	45.25	34.17	50.48	17.02	29.58	24.75	42.32	28.23	47.33	14.32	27.29
	Ours	**31.77**	**49.77**	**36.14**	**54.85**	**18.67**	**34.55**	**26.36**	**46.13**	**29.91**	**51.11**	**15.71**	**31.19**
2	Mask-DeFRCN† [21]	25.42	38.31	31.06	45.82	8.52	15.79	21.09	35.92	25.61	43.03	7.54	14.59
	Ours	**28.63**	**44.74**	**34.67**	**52.82**	**10.52**	**20.49**	**23.73**	**41.49**	**28.52**	**49.12**	**9.38**	**18.62**
3	Mask-DeFRCN† [21]	26.54	40.01	31.77	46.83	10.87	19.55	22.04	37.48	26.22	43.95	9.48	18.06
	Ours	**29.59**	**46.21**	**35.07**	**53.30**	**13.15**	**24.95**	**24.55**	**42.81**	**28.91**	**49.61**	**11.46**	**22.43**
30	Mask-DeFRCN† [21]	31.66	48.11	35.10	52.01	21.33	36.44	26.23	44.97	29.12	48.82	17.57	33.42
	Ours	**32.92**	**51.37**	**36.45**	**55.05**	**22.30**	**40.31**	**27.31**	**47.61**	**30.32**	**51.41**	**18.29**	**36.22**

on MS-COCO are reported in Table 1 and 2 for FSIS or gFSIS, respectively. Based on the experiment results, we have the following observations: **1)** The strong baseline (i.e., Mask-DeFRCN) outperforms all the state-of-the-art methods for FSIS and gFSIS; **2)** Our method consistently outperforms the baseline Mask-DeFRCN for FSIS; Compared to FSIS, our method has significant improvements for gFSIS. This is not surprised because the missing rate of gFSIS always is higher than that of FSIS as shown in Fig. 1 (b). This indicates our method is capable of addressing the missing label issue in the few-shot setting; **3)** Our method has a better advantage, especially in low-shot (1-, 2-, 3-shot), and thus it is very suitable for a few-shot scenario.

On one hand, the missing rate of low-shot is generally higher than that of high-shot so that it leaves more improvement space for our method. On the other hand, common few-shot models may be weak against noisy negative samples when the number of positive training samples is very small under the few-shot conditions. In contrast, our model is designed to deal with noisy negative samples issue, and thus it is more effective. In short, the proposed decoupling classifier is a promising approach to cope with the missing labels issue for FSIS/gFSIS.

Few-shot Object Detection on the PASCAL VOC and MS-COCO. *Our method significantly outperforms the state-of-the-art few-shot object detection methods by a large margin both on the PASCAL VOC and MS-COCO datasets under*

Table 5: FSOD performance (AP) for Novel classes on MS-COCO. Note that the superscript $*$ indicates that the results are averaged over 10 times repeated runs on `seed0`. The superscripts x indicate that the results are reported in DeFRCN [21].

Methods / Shots		1	2	3	5	10	30
FRCN-ft [31]	*ICCV 19*	1.0	1.8	2.8	4.0	6.5	11.1
FSRW [14]	*ICCV 19*	-	-	-	-	5.6	9.1
MetaDet [27]	*ICCV 19*	-	-	-	-	7.1	11.3
MetaRCNN [31]	*ICCV 19*	-	-	-	-	8.7	12.4
TFA [26]	*ICML 20*	4.4	5.4	6.0	7.7	10.0	13.7
MPSR [28]	*ECCV 20*	5.1	6.7	7.4	8.7	9.8	14.1
FSDetView [30]	*ICCV 20*	4.5	6.6	7.2	10.7	12.5	14.7
TIP [15]	*CVPR 21*	-	-	-	-	16.3	18.3
DCNet [13]	*CVPR 21*	-	-	-	-	12.8	18.6
CME [16]	*CVPR 21*	-	-	-	-	15.1	16.9
FSCE [25]	*CVPR 21*	-	-	-	-	11.1	15.3
SRR-FSD [32]	*CVPR 21*	-	-	-	-	11.3	14.7
FADI [1]	*NeurIPS 21*	5.7	7.0	8.6	10.1	12.2	16.1
FCT [10]	*CVPR 22*	5.1	7.2	9.8	12.0	15.3	20.2
DeFRCN† [21]	*ICCV 21*	7.7	11.4	13.3	15.5	18.5	22.5
Ours		**8.1**	**12.1**	**14.4**	**16.6**	**19.5**	**22.7**
DeFRCN * [21]	*ICCV 21*	9.3	12.9	**14.8**	**16.1**	**18.5**	**22.6**
Ours *		**10.0**	**13.6**	14.7	15.7	18.0	22.2

Table 3: FSOD and gFSOD performance (AP_{50}) for Novel classes on PASCAL VOC. The term *w/g* indicates whether we use the gFSOD setting [26]. Note that the superscript $*$ indicates that the results are averaged over 10 times repeated runs on `seed0`, the same below.

Methods / Shots		*w/g*	Novel Set 1					Novel Set 2					Novel Set 3				
			1	2	3	5	10	1	2	3	5	10	1	2	3	5	10
FRCN-ft [31]	*ICCV 19*	✗	13.8	19.6	32.8	41.5	45.6	7.9	15.3	26.2	31.6	39.1	9.8	11.3	19.1	35.0	45.1
FSRW [14]	*ICCV 19*	✗	14.8	15.5	26.7	33.9	47.2	15.7	15.2	22.7	30.1	40.5	21.3	25.6	28.4	42.8	45.9
MetaDet [27]	*ICCV 19*	✗	18.9	20.6	30.2	36.8	49.6	21.8	23.1	27.8	31.7	43.0	20.6	23.9	29.4	43.9	44.1
MetaRCNN [31]	*ICCV 19*	✗	19.9	25.5	35.0	45.7	51.5	10.4	19.4	29.6	34.8	45.4	14.3	18.2	27.5	41.2	48.1
TFA [26]	*ICML 20*	✗	39.8	36.1	44.7	55.7	56.0	23.5	26.9	34.1	35.1	39.1	30.8	34.8	42.8	49.5	49.8
MPSR [28]	*ECCV 20*	✗	41.7	-	51.4	55.2	61.8	24.4	-	39.2	39.9	47.8	35.6	-	42.3	48.0	49.7
TIP [15]	*CVPR 21*	✗	27.7	36.5	43.3	50.2	59.6	22.7	30.1	33.8	40.9	46.9	21.7	30.6	38.1	44.5	50.9
DCNet [13]	*CVPR 21*	✗	33.9	37.4	43.7	51.1	59.6	23.2	24.8	30.6	36.7	46.6	32.3	34.9	39.7	42.6	50.7
CME [16]	*CVPR 21*	✗	41.5	47.5	50.4	58.2	60.9	27.2	30.2	41.4	42.5	46.8	34.3	39.6	45.1	48.3	51.5
FSCE [25]	*CVPR 21*	✗	44.2	43.8	51.4	61.9	63.4	27.3	29.5	43.5	44.2	50.2	37.2	41.9	47.5	54.6	58.5
SRR-FSD [32]	*CVPR 21*	✗	47.8	50.5	51.3	55.2	56.8	32.5	35.3	39.1	40.8	43.8	40.1	41.5	44.3	46.9	46.4
FADI [1]	*NeurIPS 21*	✗	**50.3**	54.8	54.2	59.3	63.2	30.6	35.0	40.3	42.8	48.0	45.7	49.7	49.1	55.0	59.6
FCT [10]	*CVPR 22*	✗	38.5	49.6	53.5	59.8	64.3	25.9	34.2	40.1	44.9	47.4	34.7	43.9	49.3	53.1	56.3
DeFRCN† [21]	*ICCV 21*	✗	46.2	56.4	59.3	62.4	63.7	32.6	39.9	**44.5**	**48.3**	**51.8**	39.8	49.9	52.6	56.1	59.7
Ours		✗	46.2	**57.4**	**59.9**	**62.9**	**64.5**	**32.6**	**39.9**	43.4	47.9	51.3	**40.3**	**50.5**	**53.8**	**56.9**	**60.7**
DeFRCN * [21]	*ICCV 21*	✗	53.6	57.5	61.5	64.1	60.8	**30.1**	38.1	**47.0**	**53.3**	47.9	**48.4**	50.9	52.3	54.9	57.4
Ours *		✗	**56.6**	**59.6**	**62.9**	**65.6**	**62.5**	29.7	**38.7**	46.2	48.9	**48.1**	47.9	**51.9**	**53.3**	**56.1**	**59.4**
FRCN-ft [31]	*ICCV 19*	✓	9.9	15.6	21.6	28.0	52.0	9.4	13.8	17.4	21.9	39.7	8.1	13.9	19.0	23.9	44.6
FSRW [14]	*ICCV 19*	✓	14.2	23.6	29.8	36.5	35.6	12.3	19.6	25.1	31.4	29.8	12.5	21.3	26.8	33.8	31.0
TFA [26]	*ICML 20*	✓	25.3	36.4	42.1	47.9	52.8	18.3	27.5	30.9	34.1	39.5	17.9	27.2	34.3	40.8	45.6
FSDetView [30]	*ECCV 20*	✓	24.2	35.3	42.2	49.1	57.4	21.6	24.6	31.9	37.0	45.7	21.2	30.0	37.2	43.8	49.6
DeFRCN [21]	*ICCV 21*	✓	40.2	53.6	58.2	63.6	66.5	29.5	39.7	43.4	48.1	52.8	35.0	38.3	52.9	57.7	60.8
Ours		✓	**45.8**	**59.1**	**62.1**	**66.8**	**68.0**	**31.8**	**41.7**	**46.6**	**50.3**	**53.7**	**39.6**	**52.1**	**56.3**	**60.3**	**63.3**

Table 4: gFSOD performance (AP) for **O**verall, **B**ase and **N**ovel classes on MS-COCO.

Method / Shots	1			2			3			5			10			30		
	O	**B**	**N**	**O**	**B**	**N**	**O**	**B**	**N**	**O**	**B**	**N**	**O**	**B**	**N**	**O**	**B**	**N**
FRCN-ft [31]	16.2	21.0	1.7	15.8	20.0	3.1	15.0	18.8	3.7	14.4	17.6	4.6	13.4	16.1	5.5	13.5	15.6	7.4
TFA [26]	24.4	31.9	1.9	24.9	31.9	3.9	25.3	32.0	5.1	25.9	41.2	7.0	26.6	32.4	9.1	28.7	34.2	12.1
FSDetView [30]			3.2			4.9			6.7			8.1			10.7			15.9
DeFRCN [21]	24.4	30.4	4.8	25.7	31.4	8.5	26.6	32.1	10.7	27.8	32.6	13.6	29.7	34.0	16.8	31.4	34.8	21.2
Ours	**27.4**	**34.4**	**6.2**	**28.6**	**34.7**	**10.4**	**29.4**	**34.9**	**12.9**	**30.2**	**35.0**	**15.7**	**31.4**	**35.7**	**18.3**	**32.3**	**35.8**	**21.9**

gFSOD setting again. For the FSOD setting, our method is also better than the state-of-the-art in most cases. The results on the PASCAL VOC and MS-COCO are reported Tables 3, 5 and 4, respectively. Some interesting observations are summarized as follows: **1)** Our method significantly and consistently exceeds the current state-of-the-art DeFRCN under the gFSOD setting both on the PASCAL VOC and MS-COCO, which is similar to that of the gFSIS; **2)** Our method is better than the strong DeFRCN in all shots on the MS-COCO and in most cases on the PASCAL VOC under the FSOD setting (averaging the results on 10 seeds). It is worth noting that our method's performance on the MS-COCO is close (maybe slightly worse, about 0.5%) to that of DeFRCN if we compare the results based on 10 times repeated runs on the `seed0`. We recheck the missing rate of the `seed0` on the MS-COCO, and find that its corresponding missing rate is significantly different from the other 9 seeds. For example, the missing rate is 37.5%, 37.5%, 25.9%, 19.4%, 0.0%, and 0.0% for 1-, 2-, 3-, 5-, 10-, 30-shot under the FSOD setting, which is significantly lowered than that of all the 10 seeds in Fig. 1 (b). On the other hand, this also indicates that our method is robust when the missing rate is small even zero.

4.3 Ablation Study and Analysis

We conduct the ablation study to analyze the component of our method. Models in this section are based on the gFSIS setting (1-, 5-, 10-shot) using MS-COCO dataset. Note that the DeFRCN uses a Prototypical Calibration Block (PCB) to refine the classification score which is effective for improving the FSOD performance, but this brings additional computation cost. Therefore, we consider these two factors including our DC head and the PCB in the following analysis.

Effectiveness. We only simply replace the standard classifier with the proposed decoupling classifier in DeFRCN, which results in significant improvements, especially for the higher missing rate (e.g., low shot on MS-COCO). What's more, our decoupling classifier is effective not only on novel classes but also on base classes, while the PCB seems only effective on novel classes. In addition, our

Table 6: The effects of DC and PCB for gFSIS performance (AP and AP50) on MS-COCO. GFLOPs are averaged over all 5000 MS-COCO validation images.

Shots	M-Rate	DC	PCB	Complexity		Detection				Segmentation			
				#Params.	GFLOPs	Base		Novel		Base		Novel	
						AP	AP50	AP	AP50	AP	AP50	AP	AP50
1	83.3%	✗	✗	54.9M	334.54	30.09	44.45	3.89	7.43	24.62	41.58	3.52	6.88
		✓	✗	54.9M	334.54	34.35	52.46	5.04	10.03	28.03	48.60	4.59	9.12
		✗	✓	99.4M	377.88	30.11	44.42	4.95	9.55	24.63	41.57	4.45	8.81
		✓	✓	99.4M	377.88	**34.35**	**52.46**	**6.34**	**12.79**	**28.03**	**48.60**	**5.72**	**11.53**
5	80.3%	✗	✗	54.9M	334.54	32.54	48.03	11.94	21.16	26.84	45.04	10.10	19.37
		✓	✗	54.9M	334.54	35.30	53.65	14.01	26.17	29.10	49.87	11.80	23.38
		✗	✓	99.4M	377.88	32.54	48.03	13.69	24.41	26.84	45.04	11.60	22.36
		✓	✓	99.4M	377.88	**35.30**	**53.65**	**16.02**	**30.05**	**29.10**	**49.87**	**13.50**	**26.86**
10	76.7%	✗	✗	54.9M	334.54	34.05	50.21	14.96	25.70	28.12	47.10	12.60	23.81
		✓	✗	54.9M	334.54	36.13	54.81	16.66	30.79	29.90	51.07	13.98	27.72
		✗	✓	99.4M	377.88	34.17	50.48	17.02	29.58	28.23	47.33	14.32	27.29
		✓	✓	99.4M	377.88	**36.14**	**54.85**	**18.67**	**34.55**	**29.91**	**51.11**	**15.71**	**31.19**

decoupling classifier without the PCB significantly outperforms the counterpart with the PCB on base classes and is also comparable on novel classes.

Efficiency. Firstly, our decoupling classifier does not introduce any additional parameters or computation costs. Secondly, our method obtains better detection and segmentation performance when using the same complexity as Mask-DeFRCN whether the PCB is used or not. Last but not least, we only need almost half of the parameters and fewer GFLOPs when removing the PCB block, and still achieve significant improvements on base classes and comparable performance on novel classes compared to Mask-DeFRCN using the PCB.

Why DC works? We have given some analysis from the perspective of gradient optimization in Sec. 3. Here, we try to discuss from the knowledge of the learned model and compared with the baseline. We may want to know whether the decoupling classifier mitigates the bias classification. To this end, we employ Recall metric to evaluate the classification head for all ground-truth foreground objects. Note that the classification head outputs a multi-class probability distribution $\hat{\boldsymbol{p}} \in R^{C+1}$. The predicted class is determined by $\mathrm{argmax}_i \hat{p}_i$. We define that an object is recalled if its prediction is not background, i.e., any foreground category. Considering that the number of each foreground category varies considerably, we also compare $\mathrm{mRecall}$ (mean the Recalls of all classes). The comparison results are shown in Fig. 3. We can see that the $\mathrm{mRecall}$ and Recall of the decoupling classifier significantly outperforms the standard one on each shot no matter FSIS or gFSIS. This indicates that our decoupling classifier is helpful to mitigate the bias classification thus boosting the FSOD and FSIS performance.

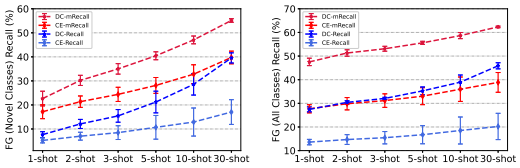

(a) FSIS (b) gFSIS

Figure 3: Comparison on $\mathrm{mRecall}$ and Recall of the proposed decoupling classifier (DC) and standard classification head (CE) under FSIS and gFSIS settings. The mean and standard deviation results are computed on all 10 seeds for each shot. Best viewed in color and zoom in.

5 Conclusion

In this paper, we firstly find that the missing label widely exists in few-shot scenario. Furthermore, we analyze that the missing label issue may result in biased classification and thus limit the generalization ability on novel classes. Therefore, we propose a simple but effective method that decouples the standard classifier into two parallel heads to independently process positive and negative examples. Comprehensive experiments on the few-shot object detection and instance segmentation benchmark datasets show that our approach can effectively and efficiently boost FSOD/gFSOD and FSIS/gFSIS performance without any additional parameters and computation cost. We hope this study attract more interest in designing a simple method for FSOD or FSIS in the future. A limitation of our method is that it may not be suitable when the missing label rate is small. However, our method is still comparable to its counterpart even if the missing label rate is zero, which indicates its robustness.

References

[1] Yuhang Cao, Jiaqi Wang, Ying Jin, Tong Wu, Kai Chen, Ziwei Liu, and Dahua Lin. Few-shot object detection via association and discrimination. In *Advances in Neural Information Processing Systems*, 2021.

[2] Liang-Chieh Chen, George Papandreou, Iasonas Kokkinos, Kevin Murphy, and Alan L Yuille. Deeplab: Semantic image segmentation with deep convolutional nets, atrous convolution, and fully connected crfs. *IEEE transactions on pattern analysis and machine intelligence*, 40(4):834–848, 2017.

[3] Jifeng Dai, Haozhi Qi, Yuwen Xiong, Yi Li, Guodong Zhang, Han Hu, and Yichen Wei. Deformable convolutional networks. In *Proceedings of the IEEE International Conference on Computer Vision*, pages 764–773, 2017.

[4] Mark Everingham, Luc Van Gool, Christopher KI Williams, John Winn, and Andrew Zisserman. The pascal visual object classes (voc) challenge. *International journal of computer vision*, 88(2):303–338, 2010.

[5] Qi Fan, Wei Zhuo, Chi-Keung Tang, and Yu-Wing Tai. Few-shot object detection with attention-rpn and multi-relation detector. In *Proceedings of the IEEE/CVF Conference on Computer Vision and Pattern Recognition*, pages 4013–4022, 2020.

[6] Zhibo Fan, Jin-Gang Yu, Zhihao Liang, Jiarong Ou, Changxin Gao, Gui-Song Xia, and Yuanqing Li. Fgn: Fully guided network for few-shot instance segmentation. In *Proceedings of the IEEE/CVF conference on computer vision and pattern recognition*, pages 9172–9181, 2020.

[7] Michael Fink. Object classification from a single example utilizing class relevance metrics. In *Advances in neural information processing systems*, 2004.

[8] Dan Andrei Ganea, Bas Boom, and Ronald Poppe. Incremental few-shot instance segmentation. In *Proceedings of the IEEE/CVF Conference on Computer Vision and Pattern Recognition*, pages 1185–1194, 2021.

[9] Ross Girshick. Fast r-cnn. In *Proceedings of the IEEE International Conference on Computer Vision*, pages 1440–1448, 2015.

[10] Guangxing Han, Jiawei Ma, Shiyuan Huang, Long Chen, and Shih-Fu Chang. Few-shot object detection with fully cross-transformer. In *Proceedings of the IEEE/CVF Conference on Computer Vision and Pattern Recognition*, 2022.

[11] Kaiming He, Georgia Gkioxari, Piotr Dollár, and Ross Girshick. Mask r-cnn. In *Proceedings of the IEEE International Conference on Computer Vision*, pages 2961–2969, 2017.

[12] Kaiming He, Xiangyu Zhang, Shaoqing Ren, and Jian Sun. Deep residual learning for image recognition. In *Proceedings of the IEEE Conference on Computer Vision and Pattern Recognition*, pages 770–778, 2016.

[13] Hanzhe Hu, Shuai Bai, Aoxue Li, Jinshi Cui, and Liwei Wang. Dense relation distillation with context-aware aggregation for few-shot object detection. In *Proceedings of the IEEE/CVF Conference on Computer Vision and Pattern Recognition*, pages 10185–10194, 2021.

[14] Bingyi Kang, Zhuang Liu, Xin Wang, Fisher Yu, Jiashi Feng, and Trevor Darrell. Few-shot object detection via feature reweighting. In *Proceedings of the IEEE International Conference on Computer Vision*, pages 8420–8429, 2019.

[15] Aoxue Li and Zhenguo Li. Transformation invariant few-shot object detection. In *Proceedings of the IEEE/CVF Conference on Computer Vision and Pattern Recognition*, pages 3094–3102, 2021.

[16] Bohao Li, Boyu Yang, Chang Liu, Feng Liu, Rongrong Ji, and Qixiang Ye. Beyond max-margin: Class margin equilibrium for few-shot object detection. In *Proceedings of the IEEE/CVF Conference on Computer Vision and Pattern Recognition*, pages 7363–7372, 2021.

[17] Tsung-Yi Lin, Michael Maire, Serge Belongie, James Hays, Pietro Perona, Deva Ramanan, Piotr Dollár, and C Lawrence Zitnick. Microsoft coco: Common objects in context. In *Proceedings of the European Conference on Computer Vision*, pages 740–755. Springer, 2014.

[18] Jonathan Long, Evan Shelhamer, and Trevor Darrell. Fully convolutional networks for semantic segmentation. In *Proceedings of the IEEE conference on computer vision and pattern recognition*, pages 3431–3440, 2015.

[19] Claudio Michaelis, Ivan Ustyuzhaninov, Matthias Bethge, and Alexander S Ecker. One-shot instance segmentation. *arXiv preprint arXiv:1811.11507*, 2018.

[20] Khoi Nguyen and Sinisa Todorovic. Fapis: A few-shot anchor-free part-based instance segmenter. In *Proceedings of the IEEE/CVF Conference on Computer Vision and Pattern Recognition*, pages 11099–11108, 2021.

[21] Limeng Qiao, Yuxuan Zhao, Zhiyuan Li, Xi Qiu, Jianan Wu, and Chi Zhang. Defrcn: Decoupled faster r-cnn for few-shot object detection. In *Proceedings of the IEEE/CVF International Conference on Computer Vision*, pages 8681–8690, 2021.

[22] Siyuan Qiao, Chenxi Liu, Wei Shen, and Alan L Yuille. Few-shot image recognition by predicting parameters from activations. In *Proceedings of the IEEE Conference on Computer Vision and Pattern Recognition*, pages 7229–7238, 2018.

[23] Joseph Redmon and Ali Farhadi. Yolo9000: better, faster, stronger. In *Proceedings of the IEEE Conference on Computer Vision and Pattern Recognition*, pages 7263–7271, 2017.

[24] Shaoqing Ren, Kaiming He, Ross Girshick, and Jian Sun. Faster r-cnn: Towards real-time object detection with region proposal networks. In *Advances in Neural Information Processing Systems*, pages 91–99, 2015.

[25] Bo Sun, Banghuai Li, Shengcai Cai, Ye Yuan, and Chi Zhang. Fsce: Few-shot object detection via contrastive proposal encoding. In *Proceedings of the IEEE/CVF Conference on Computer Vision and Pattern Recognition*, pages 7352–7362, 2021.

[26] Xin Wang, Thomas E Huang, Trevor Darrell, Joseph E Gonzalez, and Fisher Yu. Frustratingly simple few-shot object detection. In *International Conference on Machine Learning*, 2020.

[27] Yu-Xiong Wang, Deva Ramanan, and Martial Hebert. Meta-learning to detect rare objects. In *Proceedings of the IEEE International Conference on Computer Vision*, pages 9925–9934, 2019.

[28] Jiaxi Wu, Songtao Liu, Di Huang, and Yunhong Wang. Multi-scale positive sample refinement for few-shot object detection. In *Proceedings of the European Conference on Computer Vision*, pages 456–472, 2020.

[29] Yuxin Wu, Alexander Kirillov, Francisco Massa, Wan-Yen Lo, and Ross Girshick. Detectron2. `https://github.com/facebookresearch/detectron2`, 2019.

[30] Yang Xiao and Renaud Marlet. Few-shot object detection and viewpoint estimation for objects in the wild. In *Proceedings of the European Conference on Computer Vision*, 2020.

[31] Xiaopeng Yan, Ziliang Chen, Anni Xu, Xiaoxi Wang, Xiaodan Liang, and Liang Lin. Meta r-cnn: Towards general solver for instance-level low-shot learning. In *Proceedings of the IEEE/CVF International Conference on Computer Vision*, pages 9577–9586, 2019.

[32] Chenchen Zhu, Fangyi Chen, Uzair Ahmed, Zhiqiang Shen, and Marios Savvides. Semantic relation reasoning for shot-stable few-shot object detection. In *Proceedings of the IEEE/CVF Conference on Computer Vision and Pattern Recognition*, pages 8782–8791, 2021.

Checklist

1. For all authors...
   (a) Do the main claims made in the abstract and introduction accurately reflect the paper's contributions and scope? [Yes]
   (b) Did you describe the limitations of your work? [Yes] See Section 5.
   (c) Did you discuss any potential negative societal impacts of your work? [N/A]
   (d) Have you read the ethics review guidelines and ensured that your paper conforms to them? [Yes]
2. If you are including theoretical results...
   (a) Did you state the full set of assumptions of all theoretical results? [N/A]
   (b) Did you include complete proofs of all theoretical results? [N/A]
3. If you ran experiments...
   (a) Did you include the code, data, and instructions needed to reproduce the main experimental results (either in the supplemental material or as a URL)? [No] We will release the code to ensure strict reproducibility upon the paper accepted.
   (b) Did you specify all the training details (e.g., data splits, hyperparameters, how they were chosen)? [Yes] See Section 4.1.
   (c) Did you report error bars (e.g., with respect to the random seed after running experiments multiple times)? [Yes] See Fig. 3, and Appendix.
   (d) Did you include the total amount of compute and the type of resources used (e.g., type of GPUs, internal cluster, or cloud provider)? [Yes] See Section 4.1.
4. If you are using existing assets (e.g., code, data, models) or curating/releasing new assets...
   (a) If your work uses existing assets, did you cite the creators? [Yes] PASCAL VOC [4], MS-COCO [17], Detectron2 [29]
   (b) Did you mention the license of the assets? [No]
   (c) Did you include any new assets either in the supplemental material or as a URL? [No]
   (d) Did you discuss whether and how consent was obtained from people whose data you're using/curating? [No]
   (e) Did you discuss whether the data you are using/curating contains personally identifiable information or offensive content? [No]
5. If you used crowdsourcing or conducted research with human subjects...
   (a) Did you include the full text of instructions given to participants and screenshots, if applicable? [N/A]
   (b) Did you describe any potential participant risks, with links to Institutional Review Board (IRB) approvals, if applicable? [N/A]
   (c) Did you include the estimated hourly wage paid to participants and the total amount spent on participant compensation? [N/A]